

1 **A new model explaining the origin of different topologies in** 2 **interaction networks**

3 Rafael B. P. Pinheiro ^{1*}, Gabriel M. F. Félix ², Carsten F. Dormann ³, and Marco A. R.
4 Mello ^{1,4}

5

6 ¹ Graduate School in Ecology, Conservation and Wildlife Management, Federal University of Minas
7 Gerais, Brazil.

8 ² Graduate School in Ecology, State University of Campinas, Brazil.

9 ³ Department of Biometry and Environmental System Analysis, University of Freiburg, Germany.

10 ⁴ Department of Ecology, University of São Paulo, Brazil.

11 * Corresponding author. E-mail: rafael-bpp@hotmail.com

12

13 **Abstract**

14 The architecture of interaction networks has been extensively studied in the past
15 decades, and different topologies have been observed in natural systems. Despite
16 several phenomenological explanations proposed, we still understand little of the
17 mechanisms that generate those topologies. Here we present a mechanistic model based
18 on the integrative hypothesis of specialization, which aims at explaining the emergence
19 of topology and specialization in consumer-resource networks. By following three first-
20 principles and adjusting five parameters, our model was able to generate synthetic
21 weighted networks that show the main patterns of topology and specialization observed
22 in nature. Our results prove that topology emergence is possible without network-level
23 selection. In our simulations, the intensity of trade-offs in the performance of each
24 consumer species on different resource species is the main factor driving network
25 topology. We predict that interaction networks with low species diversity and low
26 dissimilarity between resources should have a nested topology, although more diverse
27 networks with large dissimilarity should have a compound topology. Additionally, our
28 results highlight scale as a key factor. Our model generates predictions consistent with
29 ecological and evolutionary theories and real-world observations. Therefore, it supports
30 the IHS as a useful conceptual framework to study the architecture of interaction
31 networks.

32 **Keywords:** Ecological interactions; interaction networks; consumer-resource networks;
33 network topology; nestedness; modularity; compound topology; specialization; trade-
34 offs;

35

36 Introduction

37 In the past decades, network science, by focusing on the structure of entire systems
38 instead of species, proved to be an outstanding tool for the study of ecological
39 interactions (Dormann *et al.* 2017). One persisting controversy in the literature is the
40 predominant architecture among interaction networks. Two main topologies have been
41 proposed as almost universal: nested and modular (Fortuna *et al.* 2010).

42 Several studies have detected significant nestedness in interaction networks (Bascompte
43 *et al.* 2003; Guimarães *et al.* 2007b). In a perfectly nested network, the links (i.e.,
44 connection between two species in a network) made by species with fewer interaction
45 partners (i.e., other species to which it is connected) tend to be a subset of the links
46 made by species with more interaction partners (Bascompte & Jordano 2007), so
47 interaction overlap is maximum. Nevertheless, several other studies have found a
48 modular topology in interaction networks. A modular network is composed of
49 subgroups of densely connected species (Guimerà *et al.* 2010; Bellay *et al.* 2011; Watts
50 *et al.* 2016).

51 Contrary to nestedness, modularity is characterized by each node interacting
52 preferentially with a particular subgroup of nodes, overlap is reduced, and several links
53 are considered forbidden (e.g., impossible to occur due to trait mismatch, Jordano
54 2016). Usually, modules are composed of phylogenetically close species (Krasnov *et al.*
55 2012) or species that converge in a set of traits (Mello *et al.* 2011). Despite nestedness
56 and modularity being logically different topologies (Ulrich *et al.* 2017) and usually
57 negatively correlated with one another in empirical ecological networks (Thebault &
58 Fontaine 2010; Pires & Guimaraes 2012; Trøjelsgaard & Olesen 2013), networks
59 combining some degree of both have been observed in nature (Olesen *et al.* 2007;
60 Bellay *et al.* 2011; Flores *et al.* 2013).

61 Diverse explanations to the emergence of each network topology have been proposed
62 For instance, interactions driven by abundance (Vázquez *et al.* 2007), neutrality
63 (Krishna *et al.* 2008), and morphological constrains (Stang *et al.* 2007) for nestedness.
64 And phylogenetic conservatism (Krasnov *et al.* 2012), functional complementarity
65 (Montoya *et al.* 2015), and trait-matching (Donatti *et al.* 2011) for modularity.
66 Interaction intimacy does also seem to play a role in shaping network topology (Hembry
67 *et al.* 2018).

68 Additionally, a recurrent hypothesis is that nestedness should be expected in mutualisms
69 while modularity should emerge in antagonisms (Thebault & Fontaine 2010).
70 Nevertheless, several studies found empirical evidence against this hypothesis (Olesen
71 *et al.* 2007; Mello *et al.* 2011; Pires & Guimaraes 2012). Despite a diversity of
72 phenomenological explanations, we still poorly understand the mechanisms that drives
73 the establishment of links and so shape network architecture, an issue already pointed
74 out (Ings *et al.* 2009), but which still has not been properly addressed. Maybe as a
75 symptom of this knowledge gap, community-level selection is commonly invoked to

76 explain interaction network topology, despite the strong criticism against it in the
77 evolutionary literature (see Pires & Guimaraes 2012). In the present study, we use a
78 recent hypothesis to propose a unified mechanism that drives the formation of links and
79 scales up to shape network topology.

80 The integrative hypothesis of specialization (IHS), (early called the integrative
81 hypothesis of parasite specialization, Pinheiro *et al.* 2016; Felix *et al.* 2017), is aimed at
82 explaining the relationship between performance and specialization in consumer-
83 resource interactions (e.g., parasite-host, prey-predator, plant-pollinator). A classical
84 hypothesis states that, due to trade-offs involved in specialization, generalist consumers
85 should be outperformed by specialist consumers in exploiting each resource (Futuyma
86 & Moreno 1988). It is illustrated by the figure of speech “jack-of-all-trades, master of
87 none”. In this scenario, because of those trade-offs, each consumer species tends to
88 specialize in one or few resource species, and several interactions are forbidden. Indeed,
89 some studies have found compelling evidence corroborating this hypothesis in different
90 systems (Poulin 1998; Muchhala 2007). However, other studies found that generalistic
91 consumers achieve higher performance in exploiting each resource (Krasnov *et al.*
92 2004; García-Robledo & Horvitz 2012). In such cases there is no generalism-
93 performance trade-off and specialization is a sub-optimal state for a consumer. The IHS
94 was initially proposed as an explanation for this diversity of results.

95 The main question behind this dilemma is whether the same traits that allow a consumer
96 species to efficiently exploit a given resource species do also allow it to exploit other
97 resource species. This tends to be true if the resources are similar to one another, but
98 false if not (Krasnov *et al.* 2004). Starting from this perspective, the IHS predicts that
99 the relationship between consumer’s performance and specialization depends on
100 resource heterogeneity. However, diverse communities can comprise clusters of similar
101 resource species, each cluster being highly different from the other. For instance, the
102 host community studied by Pinheiro *et al.* (2016) contains several birds species of the
103 same genus, but also birds of different orders. In such cases of a wide range of resource
104 dissimilarities, the IHS predicts a multi-scale relationship between performance and
105 specialization. Considering only a group of similar resources, a “jack-of-all-trades”
106 consumer tends to be master of all, though, between different clusters of resources the
107 trade-off is strong (Pinheiro *et al.* 2016).

108 In previous studies, we proposed that the same mechanism governing the specialization
109 vs. performance relationship may drive the architecture of consumer-resource networks
110 (Pinheiro *et al.* 2016; Felix *et al.* 2017). From this perspective, nestedness is the result
111 of the correlated performances of each consumer on similar resources, although
112 modularity emerges because of strong trade-offs in performances on dissimilar
113 resources. Therefore, the IHS predicts that subnetworks that represent phylogenetic or
114 taxonomic subsets of complete systems, and thus do not comprise trade-offs, should be
115 nested. However, in more diverse networks a multi-scale topology should emerge: a
116 modular structure with internally nested modules.

117 This multi-scale architecture was named compound topology, a conceptual archetype
118 proposed by Lewinsohn *et al.* (2006) and predicted by Flores *et al.* (2011). A compound
119 topology is also a suitable explanation for networks that are nested and modular at the
120 same time, because in those networks those conflicting topologies would predominate at
121 different scales, instead of being mixed in the structure (as suggested by Fortuna *et al.*
122 2010). Evidence of a compound topology was found in pollination (Bezerra *et al.* 2009),
123 bacteria-phage (Flores *et al.* 2013), and mammal-flea (Felix *et al.* 2017) empirical
124 networks, as well as in synthetic networks (Beckett & Williams 2013; Leung & Weitz
125 2016). Moreover, a pattern of in-block nestedness was found in a large set of
126 mutualistic and antagonistic networks, which, as far as we can tell, is the same structure
127 as a compound topology (Solé-Ribalta *et al.* 2018).

128 Here, we propose a new mechanistic model for interaction networks based on the IHS.
129 Our new model is presented in terms of consumers and resources, so it can help predict
130 the topology of networks formed by different kinds of interaction, from antagonism to
131 mutualism. The first-principles of our model are: (i) each resource species has a set of
132 traits that affect its exploitability by each consumer species, and resource species can be
133 more or less similar to one another in those traits; (ii) a consumer's mutation that
134 enhances its exploitation of a given resource tends to improve the exploitation of similar
135 resources, but worsen its exploitation of dissimilar resources; and (iii) the capacity of a
136 consumer to exploit each resource on a given moment is a result of its previous
137 adaptations and maladaptations.

138 Following these simple principles, and adjusting a set of five parameters, we tested
139 whether the IHS model can: (1) reproduce the varied relationships between performance
140 and specialization of consumers observed in natural systems; (2) reproduce the main
141 topologies observed in interaction networks, (3) explain the general conditions that
142 affect the emergence of those patterns, and (4) generate predictions that are consistent
143 with ecological and evolutionary theories and coherent with real-world observations.
144 Moreover, our model is aimed to be a proof-of-concept (*sensu* Servedio *et al.* 2014) of
145 the IHS, testing whether its predictions are logically derived from its assumptions and
146 mechanism.

147 **The IHS model**

148 Core structure

149 Our model simulates the evolution of consumer species exploiting resource species. It is
150 species-based and does not account for intraspecific variations. For increased text
151 fluency, hereafter, we call consumer species “consumers” and resource species
152 “resources”. Similarly, consumer species richness is referred to as “consumer richness”,
153 and resource species richness as “resource richness”.

154 The core of our model consists of two evolving matrices: the innate performance
155 matrix, and the realized performance matrix. In addition, there are two static inputs: a

156 matrix with the pairwise distances between resources, and a vector of resource carrying
157 capacities (Fig. 1).

158 Innate performance represents the match between a consumer and a resource. It
159 summarizes how all characteristics of the consumer (e.g., morphology, physiology, and
160 behavior) affect its ability to exploit a given resource. When a consumer has a negative
161 innate performance on a resource, it is incapable of exploiting it. However, when its
162 innate performance is positive, the consumer exploits the resource (has a realized
163 performance on it).

164 The distance between two resources in our model is a measure of how different they are
165 from consumer's perspective. Resources are close to one another when they require of
166 the consumers the same adaptations for an efficient exploitation. For instance, two plant
167 species, whose fruits have similar shape, size, and consistency, require from frugivorous
168 birds the same type of beak. Resources are distant from one another when they require
169 of the consumers opposite adaptations for an efficient exploitation. For instance, two
170 plant species whose fruits are more easily consumed by, respectively, small-beaked and
171 large-beaked birds. Because of phylogenetic conservatism, we expect the distances
172 between resources to mirror the taxonomic and phylogenetic distances between them,
173 however, convergence may confuse this pattern.

174 The carrying capacity of each resource limits the overall realized performance of its
175 consumers. It can be understood as the availability of each resource for consumer
176 exploitation. In natural systems, we expect abundance, size, and vulnerability (in
177 antagonisms) or accessibility (in mutualisms) of each resource to be major factors
178 defining this value.

179 Each realized performance represents the strength of an interaction effectively made in
180 a consumer-resource system, therefore it cannot have a negative value. It integrates the
181 match between consumers and resources (i.e., innate performance) with the limitations
182 imposed by each resource carrying capacity, as presented in equation 1:

$$183 \quad RP_{ij} = \begin{cases} \frac{IP_{ij}}{\sum_{i=1}^{S_c} IP_{ij}} K_j, & \text{if } IP_{ij} \geq 0 \\ 0, & \text{if } IP_{ij} < 0 \end{cases} \quad (1)$$

184 in which IP_{ij} is the innate performance of consumer i on resource j , RP_{ij} is the realized
185 performance of consumer i on resource j , S_c is consumer richness, and K_j is the
186 carrying capacity of resource j . In other words, consumers that have negative innate
187 performances on a given resource, have zero realized performance on it. And for
188 consumers that have positive innate performances on a given resource, the realized
189 performances are the resource's carrying capacity divided between these consumers
190 proportionally to their innate performances.

191 Mutation phase

192 At the beginning of each iteration, a consumer is randomly assigned to evolve. This
193 consumer, then, is submitted to alternative mutations, one focused on each resource
194 (focal resource), therefore generating S_r (resource richness) mutants of the consumer.

195 Mutations change the innate performance of the assigned consumer on all resources.
196 The values of those changes are randomly drawn from normal distributions, in which
197 standards deviations are equal to 0.3 and means are defined by the distance between
198 each resource and the focal resource of the mutation, as presented in equation 2:

199
$$\mu_j = 1 - \alpha_{jf} \quad (2)$$

200 in which μ_j is the mean of the normal distribution from which we draw the value of
201 changes in the innate performance of the assigned consumer on resource j , and α_{jf} is
202 the distance between resource j and the focal resource f . Since the distance of the focal
203 resource from itself is 0, the focal mutation will be a value randomly drawn from a
204 normal distribution of mean = 1. Notice that, as a consequence of equation 3, each
205 mutation probabilistically tends to increase the innate performance of the mutating
206 consumer on resources with distances from the focal resource above 1 ($\mu_j > 0$) and
207 tends to decrease performances beyond this threshold ($\mu_j < 0$).

208 Selection phase

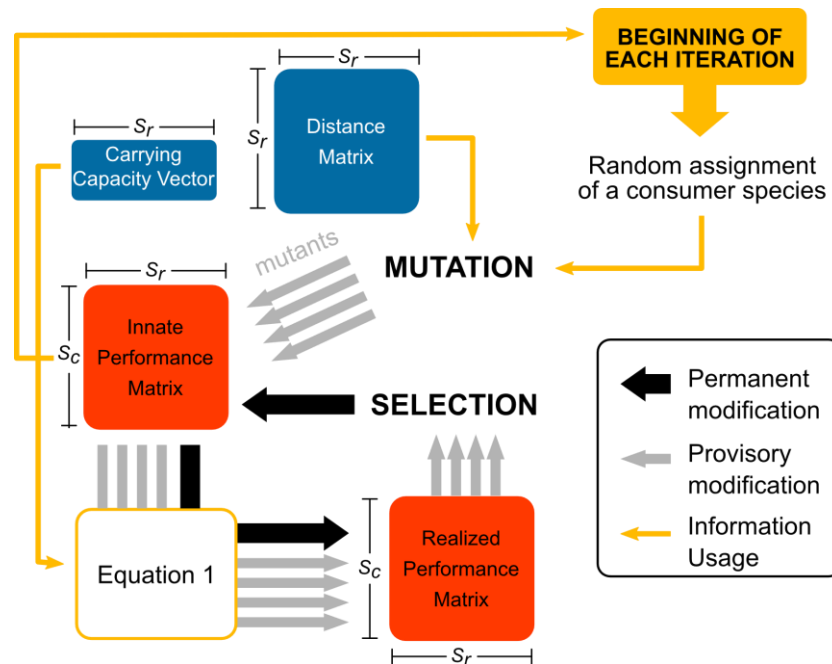
209 In the selection phase, following equation 1, the total realized performance of each
210 mutant consumer is compared with the total realized performance of the original
211 consumer (before mutations). If at least one mutant present increased total realized
212 performance, the mutant with the largest total realized performance is selected,
213 replacing the original consumer in the innate performance matrix for the next iteration
214 (i.e., evolutionary changes occurred). However, if all mutations result in decreased total
215 realized performance, the original consumer is selected, and the simulation goes to the
216 next iteration without evolutionary changes.

217 End of the simulation

218 The simulation ends after a pre-defined number of iterations. Then, by applying
219 equation 1 on the final innate performance matrix, the final realized performance matrix
220 is generated. This matrix corresponds to the simulated consumer-resource network
221 (hereafter referred to as “simulated network”). Its contains the information concerning
222 the consumer and resource species in the network (nodes), the interactions that are made
223 between those species: consumers exploiting resources (links), and the consumers’
224 performance on exploiting each resource (weights). Moreover, as consumers cannot
225 interact with other consumers, nor resources can interact with other resources, the
226 simulated network is bipartite (two-mode).

227 For a complete example of an iteration of the IHS model, see Fig. S1 in Supporting
 228 Information.

229



230

231 **Figure 1 – The IHS model.** The iteration starts with the assignment of a random consumer that
 232 will evolve. This consumer suffers alternative mutations, each generating a mutant with its own
 233 innate performances on resources. Each mutation is focused on a given resource (focal resource)
 234 but affects the consumer’s innate performance on all resources. The consequence of each
 235 mutation for the consumer’s innate performance on a given resource depends on the distance
 236 between this resource and the focal resource, which is given by the resource species distance
 237 matrix. Then, using equation 1 (see the section “The IHS model”) the realized performance of
 238 each mutant is calculated. The mutant with the highest total realized performance is selected
 239 and replaces the original consumer in the innate performance matrix to be used in the next
 240 iteration of the model (unless all mutations result in decreased total realized performance, in
 241 which case the original consumer is maintained). For a detailed example of one iteration of
 242 the IHS model see Supplementary Figure S1. S_c : consumer richness; S_r : resource richness. Elements
 243 in blue are static inputs: do not change during the simulation. Elements in red are evolving
 matrices.

244

245 Simulations

246 Inputs and parameters of the simulations

247 Innate performance matrix

248 To start each simulation, we need to provide an initial innate performance matrix. We
 249 built matrices with different consumer richness and resource richness. To fill the matrix
 250 we used three different methods: rep0) all consumers score 0 (zero) in innate

251 performance on all resources, then the first mutation of a consumer corresponds to its
252 ingress in the simulated network; rnorm(1) the innate performance of each consumer on
253 each resource is randomly drawn from a normal distribution with mean = 1 and standard
254 deviation = 1; and rep(1) all consumers score 1 (one) in innate performance on all
255 resources.

256 Carrying capacity vector

257 The carrying capacity of each resource was defined by randomly drawing a value from
258 a normal distribution with mean = 200 and standard deviation = 50.

259 Matrix of resource distances

260 The IHS predicts that network topology emerges as a function of the distance between
261 resources and the degree of clustering of those distances. To test this prediction, we
262 generated distance matrices defining values for the maximum distance between two
263 resources and the number of clusters it contains (for details see Supplement S1).

264 Number of iterations

265 The number of iterations for each simulation was defined as each consumer has
266 averaged 50 rounds of evolution. Therefore, the number of iterations equals consumer
267 richness times 50.

268 List of parameters

269 In our simulations we adjusted five parameters: the consumer richness, the resource
270 richness, the method used to generate the initial innate performance matrix (innate
271 method), the maximum distance between two resources (maximum distance), and the
272 number of resource clusters (number of clusters).

273 **Running simulations**

274 Simulations were coded in R (R Core Team 2018). For commented codes see
275 Supplement S1. The parameter values used in our simulations were: consumer richness:
276 5, 10, 50, 100, and 200; resource richness: 50, 100, and 200; innate method: rep(0),
277 rnorm(1), and rep(1); maximum distance: 1, 1.5, 2, 2.5, 3, 3.5, and 4; and number of
278 clusters: 1, 2, and 4. We ran one simulation for each combination of those values,
279 totalizing 945 setups.

280 **Statistical analysis**

281 **Proportion of iterations in which occurred evolutionary changes**

282 We used generalized linear models (GLM) to test which parameters affected the
283 proportion of iterations in which occurred evolutionary changes in each simulation. In
284 the complete model, we included as explanatory variables: (1) maximum distance, (2)

285 innate method, (3) number of clusters (as a categorical variable), (4) resource richness,
286 (5) consumer richness, and all interactions between variables (1), (2), and (3). After
287 building the complete model, we used a backward stepwise approach with analysis of
288 variance to reduce it to a minimum model. We used the explained deviance of each
289 explanatory variable in the minimum model as a measure of effect size. This same setup
290 was followed in all GLMs built in our study. For details about all statistical analyses
291 performed in this study see Appendix S1.

292 For the subsequent analyses, we removed the simulations in which evolutionary
293 changes occurred in less than 80% of iterations. There remained 672 simulations (72%).

294 **Relationship between performance and resource specialization of consumers**

295 For each consumer in the simulated networks we calculated three performance indices:
296 (1) mean realized performance, its average performance on all resources it exploits, (2)
297 maximum realized performance, its maximum performance on a single resource, and (3)
298 total realized performance, the sum of its performances on all resources. We also
299 calculated two resource specialization indices, the first binary and the second weighted:
300 (1) basic resource specialization, the richness of resource species exploited by the
301 consumer, and (2) structural resource specialization, the diversity of resources exploited
302 by the consumer measured with Shannon index (Poisot *et al.* 2012).

303 Then, we calculated Spearman correlations between the three performance indices and
304 the two resource specialization indices for each simulated network. It was not possible
305 to calculate the correlations using basic resource specialization for completely filled
306 matrices, because in them, all consumers exploit the same resource richness.

307 To assess which factors influence the relationship between consumers' performance and
308 specialization in our simulations, we used generalized additive models (GAM) with the
309 correlations as response variables and simulation parameters as explanatory variables.
310 The maximum distance was included as a smooth term on each GAM. To find the
311 minimum model we used the same approach used for the GLMs. In the present study,
312 we used GAMs when the relationship between the response variable and maximum
313 distance could not be properly modelled with a GLM.

314 **Network analysis**

315 Network specialization

316 For each simulated network, we calculated a binary and a weighted network
317 specialization metric: respectively, connectance and H_2' (Blüthgen *et al.* 2006).
318 Connectance is defined as the proportion of potential links that are made in the network,
319 therefore, the smaller its value, the more specialized the network. For H_2' the contrary is
320 true: the higher its value, the more specialized the network. Specialization indices were
321 computed using the package bipartite for R (Dormann *et al.* 2008). To test whether the

322 simulation parameters influenced the specialization of the simulated networks we used
323 GLMs.

324 Modularity

325 To measure the modularity and module composition of each simulated network we used
326 the DIRTLPAwb+ algorithm (Beckett 2016), which maximizes the Barber modularity
327 (Barber 2007) for weighted bipartite networks. Then we tested whether modularity
328 values were affected by simulation parameters using GLMs.

329 Nestedness

330 To compute nestedness in weighted bipartite networks we used a new metric, which we
331 named WNODA (weighted nestedness based on overlap and decreasing abundance).
332 WNODA is a modification of WNODF (weighted nestedness based on overlap and
333 decreasing fill) (Almeida-Neto & Ulrich 2011). WNODF is a nestedness metric
334 designed for weighted networks, however, it maintains the condition of binary
335 decreasing fill from the original NODF metric (Almeida-Neto *et al.* 2008). Therefore,
336 WNODF can be strongly affected by weak links, which is not optimal for a weighted
337 metric, and cannot deal with completely filled matrices (in those cases WNODF is 0).
338 WNODA, in turn, does not demand binary nestedness to account for weighted
339 nestedness, is less affected by weak links, and can be used for completely filled
340 matrices. WNODA measures how frequently the weight of each link made by a node of
341 lower total abundance is weaker than the weight of those same link made by a node
342 with higher total abundance. Detailed information about WNODA and comparisons
343 between metrics are presented in Appendix S2.

344 We calculated the WNODA of each simulated network and used GLMs to see how it
345 was affected by the simulation parameters. To test the correlation between nestedness
346 and modularity in our networks, we performed a Spearman correlation test.

347 Considering the possibility of a compound topology in our simulated networks, we used
348 an approach based on the method proposed by Flores *et al.* (2013) and adapted by Felix
349 *et al.* (2017), in which we separately compute the nestedness between species belonging
350 to the same module and the nestedness between species belonging to different modules
351 (Felix *et al.* 2017). This method can be performed with any nestedness metric based on
352 pairwise comparison between nodes, including WNODA (see Appendix S2).

353 In a network with a compound topology we expect the WNODA between species of the
354 same module ($WNODA_{SM}$) to be much higher than the WNODA between species of
355 different modules ($WNODA_{DM}$). An R function to compute these components of
356 nestedness using NODF, WNODF, and WNODA is provided in Supplement S2.

357 We used GLMs to test for effects of maximum distance and number of clusters on the
358 $WNODA_{SM}$ and $WNODA_{DM}$ of the simulated networks.

359 Network topologies

360 In the present study, we considered three network topologies: modular, nested, and
361 compound. To categorically define which topology was shown by each simulated
362 network, we used the approach proposed by Felix *et al.* (2017) based on null model
363 analysis.

364 First, we tested for nested and modular topologies using free null models. In the free
365 models, each randomized matrix was generated using a modified version of the method
366 proposed by Vázquez *et al.* (2007). Their method creates a null matrix conserving the
367 original connectance and the total number of interactions, and probabilistically
368 conserving the marginal sums. To this end, the algorithm first defines the binary
369 structure of the null matrix, assigning interactions according to probabilities based on
370 the marginal sums of the original matrix. However, to prevent reducing the size of the
371 matrix, the algorithm requires that each species makes at least one interaction. After
372 that, the remaining interactions are distributed among the filled cells, following again
373 probabilities based on marginal sums. This method, however, is not fully adequate to
374 our simulated matrices, as their interaction weights are not counts, but continuous.
375 Therefore, the procedure results in null matrices with very different marginal sums from
376 the original matrix, especially in matrices with many weak interactions. To deal with
377 this, we modified the algorithm so that it does not fill the matrices by distributing
378 unitary interactions (including and summing 1s) but by distributing a lower value. We
379 defined this value as 0.1, as this was low enough to reasonable conserve the marginal
380 sums.

381 For each simulated network, we generated a free null model with 500 randomized
382 matrices and performed a Z-test to test whether the observed value of each metric was
383 significantly different from the distribution of values of the null matrices. A network
384 was considered modular when its value of Barber Modularity was significantly higher
385 than the randomized values. Similarly, a network was considered nested, when it had a
386 significant WNODA value. To avoid excessively low consumer richness in each
387 module, we excluded the networks with 10 or fewer consumer species and kept 415
388 simulated networks for this and subsequent analysis.

389 A network was considered as having a compound topology, when it was significantly
390 modular and presented a significant $WNODA_{SM}$ (i.e., a modular network with modules
391 internally nested). To test the significance of $WNODA_{SM}$ in each simulated network we
392 used restricted null models (Felix *et al.* 2017). A restricted null model is one that
393 conserves the modular structure of the matrix when generating the randomized matrices.
394 As, by definition, nodes in the same modules overlap more than nodes in different
395 modules, not conserving the modular structure of the randomized matrix (i.e., using a
396 free null model) would result in an inflated type I error ratio for $WNODA_{SM}$.

397 In the restricted null model, each interaction is first assigned an *a priori* probability and
398 then the probabilities are adjusted to keep the modular structure. Here we used two

399 different algorithms to assign the *a priori* probabilities of each interaction: Equiprobable
400 and Degree-probable. In the Equiprobable method, *a priori* probabilities are equal for
401 all cells and, therefore, only the modular structure defines the probability of each
402 interaction. In the Degree-probable method, *a priori* probabilities are defined based on
403 marginal sums (same method used for the free null model) and then adjusted to maintain
404 the modular structure of the matrix.

405 Null model analysis was performed in the Sagarana High-Performance Computing
406 cluster from the High-Performance Processing Center, Institute of Biological Sciences,
407 Federal University of Minas Gerais, Brazil.

408 We built GLMs to test how the simulation parameters affected the chance of a
409 simulated network having a modular topology. Similarly, we tested for a nested
410 topology. Then we tested, only for modular networks, how the simulation parameters
411 affected their chances of having a compound topology.

412 **Multi-scale relationship between performance and specialization**

413 To measure the resource specialization of consumers at different network scales, for
414 each consumer in each modular network we calculated its standardized within-module
415 degree (Z) and participation coefficient (P) (Guimerà & Nunes Amaral 2005). The first
416 is a Z-score of the consumer's degree within its module, and measures within-module
417 specialization (small network scale). The second is a measure of how much the
418 consumer's links are distributed between different modules; therefore, it represents
419 between-module specialization (large network scale). We also developed weighted
420 versions of Z and P. The weighted Z is the Z-score of the diversity of links made by the
421 consumer within its module, measured with Shannon index, and the weighted P
422 measure the distribution of weights between modules.

423 As for the calculation of Z we need to compute standard deviations, it cannot be applied
424 when all nodes of a module have the same degree. This resulted in some networks
425 having too few usable values. For this analysis, we discarded networks with fewer than
426 5 nodes with meaningful values of both Z and P.

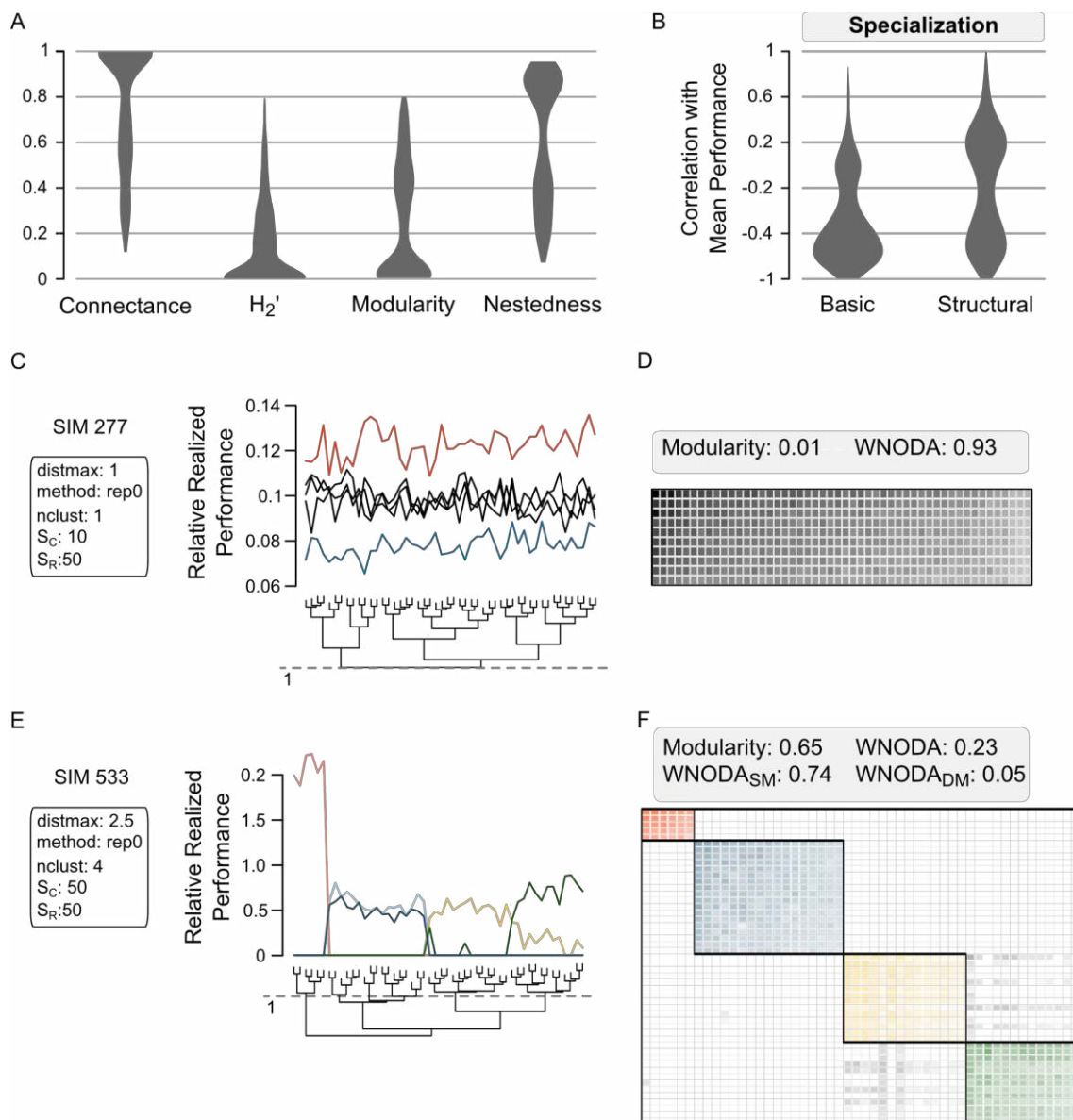
427 Then, for each network, we made linear regressions with consumer performances
428 (mean, maximum and total) as response variables, and Z and P values (binary and
429 weighted version) as explanatory variables. Finally, to test whether simulation
430 parameters affected the relationship between performance and specialization of
431 consumers at different network scales (i.e., coefficients of Z: β_Z and $\beta_{\text{Weighted-Z}}$, and
432 coefficients of P: β_P and $\beta_{\text{Weighted-P}}$ in the linear regressions), we used GAMs.

433 **Results**

434 The proportion of iterations in which occurred evolutionary changes decreased with
435 maximum distance and number of clusters, and was lower in matrices built with the

436 innate methods “rep1” and “rnorm11”. The other simulation parameters had low
 437 explanatory power (see Appendix S1.1). Out of the 945 simulations performed, 267
 438 (28%) had less than 80% of the iterations with evolutionary changes and were removed
 439 from the subsequent analyses. The remaining simulations resulted in a highly diverse
 440 set of networks for every metric calculated in this study. Fig. 2 presents examples of this
 441 large variability.

442



443

444

445 **Figure 2 - Diversity of patterns in the simulated networks.** Our simulations resulted in a
 446 highly diverse set of consumer-resource networks considering all metrics analyzed (A). The
 447 relationship between specialization and performance of consumers varied largely (B). Here we
 448 illustrate two opposite patterns of specialization using as an example the simulated networks
 449 277 (C-D) and 533 (E-F). In C and E, each line represents a consumer species. Five consumer

450 species were sorted from each simulated system and their relative realized performances were
451 plotted. The trees were obtained by hierarchical clustering of the distances between resources in
452 the simulations, using the complete linkage method. Simulation 277 does not include
453 performance trade-offs (maximum distance = 1) and does not have clusters in resource distance
454 structure. The consumer which has the highest performance in one resource, also has the highest
455 performances in all other resources (red line): the jack-of-all-trades is master of all. This
456 simulation generated a network with very high nestedness and very low modularity (D). Rows
457 and columns in D were organized by decreasing marginal sums and the grey tones represent the
458 weight of each interaction. Nestedness is evidenced by the general trend of decreasing weights
459 top-down and left-right in the matrix (D). Simulation 533 includes moderate trade-offs and
460 clusters of similar resources. In this case, each consumer specializes in a group of similar
461 resources (E). The network (F) has high modularity and low nestedness. Nevertheless,
462 nestedness between species of the same module is high.

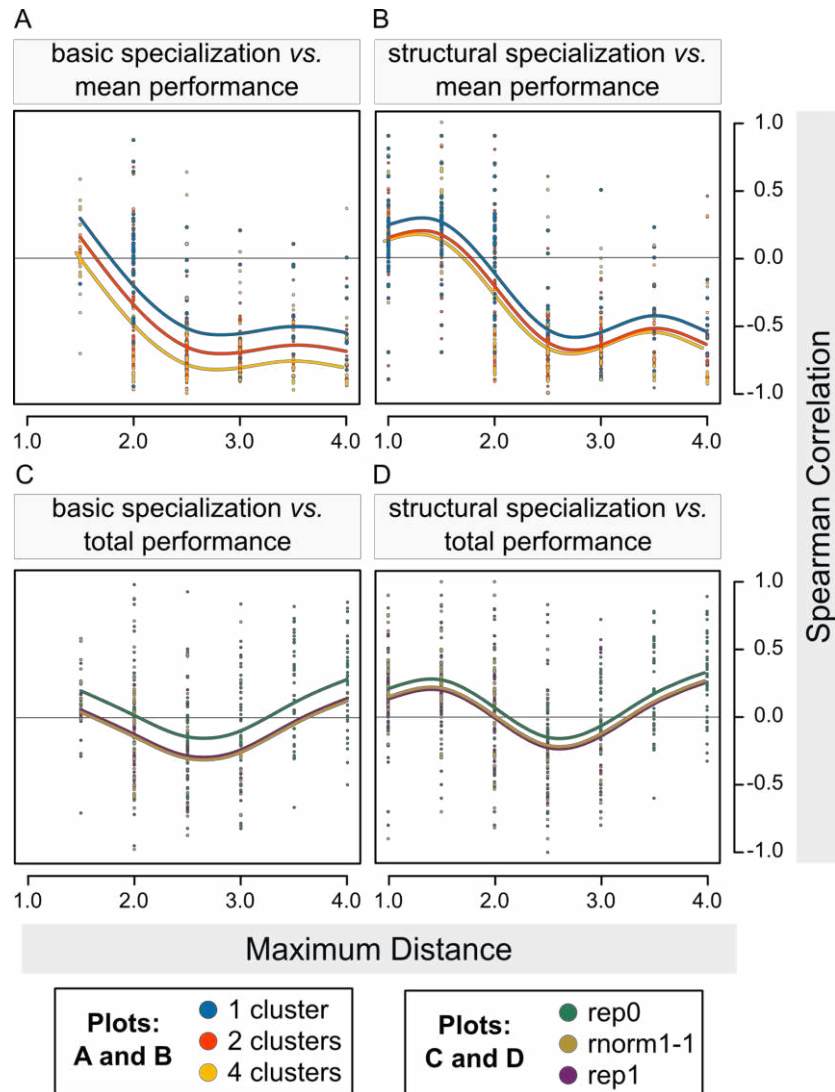
463

464 The correlation between mean performance and resource specialization depended on the
465 distance between resources and the number of resource clusters, varying from positive
466 to negative, and following the same general trend regardless of the resource
467 specialization index used (Fig. 3A-C). The same trend held for the correlations with
468 maximum performance (Appendix S1.2). The correlations involving total performance
469 varied non-linearly with maximum distance. Our model predicts that specialists will
470 present higher total performance than generalists when resources are intermediately
471 distant one from another. Otherwise, generalists outperform specialists (Fig. 3D-E). See
472 Appendix S1.2.

473 We found a consistent pattern of increasing network specialization with increasing
474 maximum distance and number of clusters in simulations, in both the GLMs with
475 connectance and H_2' (Fig. 4). Parameters related to the size of the network (consumer
476 richness and resource richness) had just minor effects on connectance, but consumer
477 richness had a moderate effect on H_2' . Although the innate method defines the
478 specialization of the initial matrix, it had little effect on connectance (Appendix S1.3)
479 and H_2' (Appendix S1.4) in the simulated networks.

480 Modularity increased with maximum distance and number of clusters (Fig. 5A), while
481 nestedness decreased with those parameters (Fig. 5B). The other parameters had little or
482 no effect on nestedness (Appendix S1.5) and modularity (Appendix S1.6) in the
483 simulated networks. Both $WNODA_{SM}$ and $WNODA_{DM}$ decreased with maximum
484 distance and number of clusters (Fig. 5C, Appendix S1.7). However, the former has a
485 smaller slope than the later, and, therefore, the expected ratio between $WNODA_{SM}$ and
486 $WNODA_{DM}$ increased with maximum distance and number of clusters (Fig. 5D). There
487 is a strong negative correlation between modularity and nestedness on the simulated
488 networks (Spearman rho: -0.94, $p < 0.001$) (Fig. 5E, Appendix S1.8).

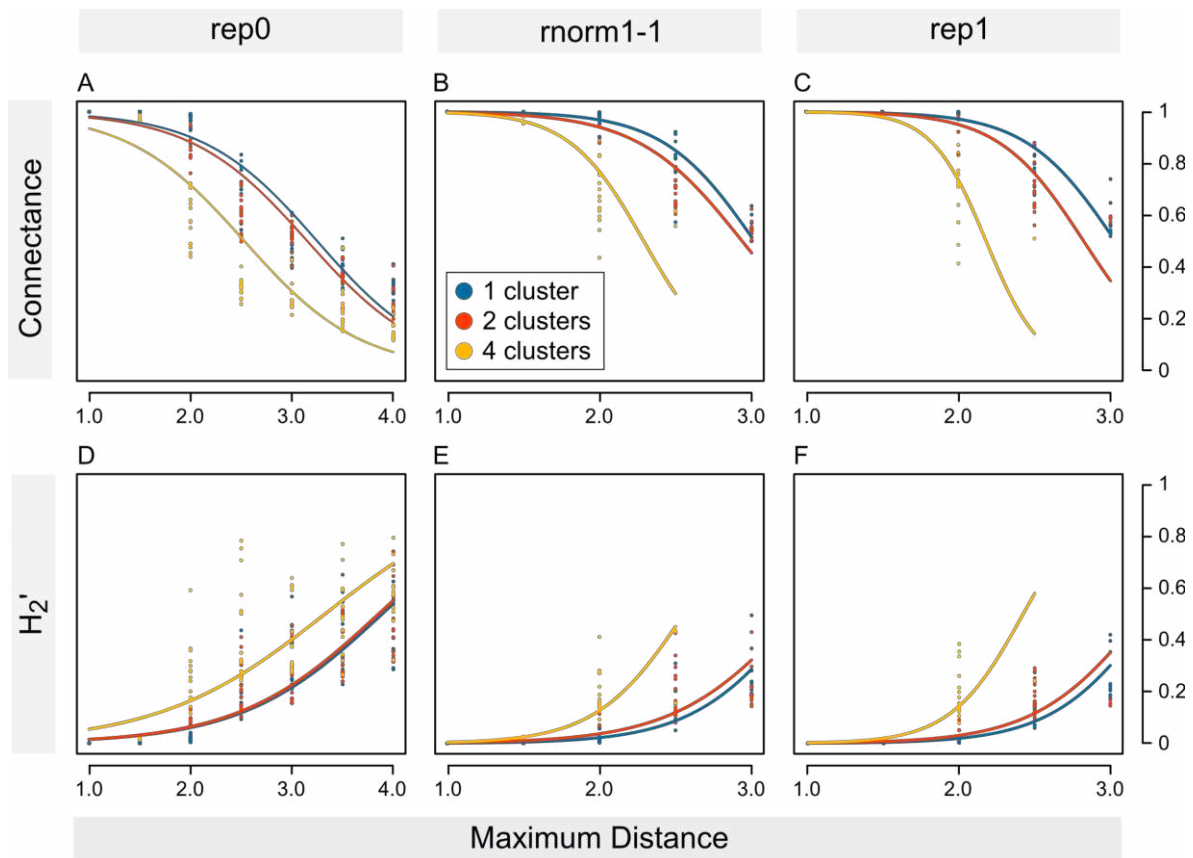
489



490

491 **Figure 3 - Correlations between performance and specialization of consumers.** Correlations
 492 in the simulated network are presented as a function of maximum distance (horizontal axis), and
 493 number of clusters (colors in plots A and B) or innate method (colors in plots C and D). For
 494 each network we calculated Spearman correlations between indices of consumers' realized
 495 performance (mean realized performance, maximum realized performance, and total realized
 496 performance) and indices of consumers' specialization (basic specialization and structural
 497 specialization). Results for maximum performance were very similar to results for mean
 498 performance and are presented in Appendix S1. Notice that the values of specialization indices
 499 are negatively related to specialization, i.e., the higher the diversity of resources exploited by a
 500 consumer, the less specialized the consumer. The parameters represented in each plot are the
 501 ones with more explanatory power in the generalized additive models (see Appendix S1.2). In
 502 all plots, when consumer or resource richness were significant explanatory variables, we used
 503 its average values to draw the curves.

504

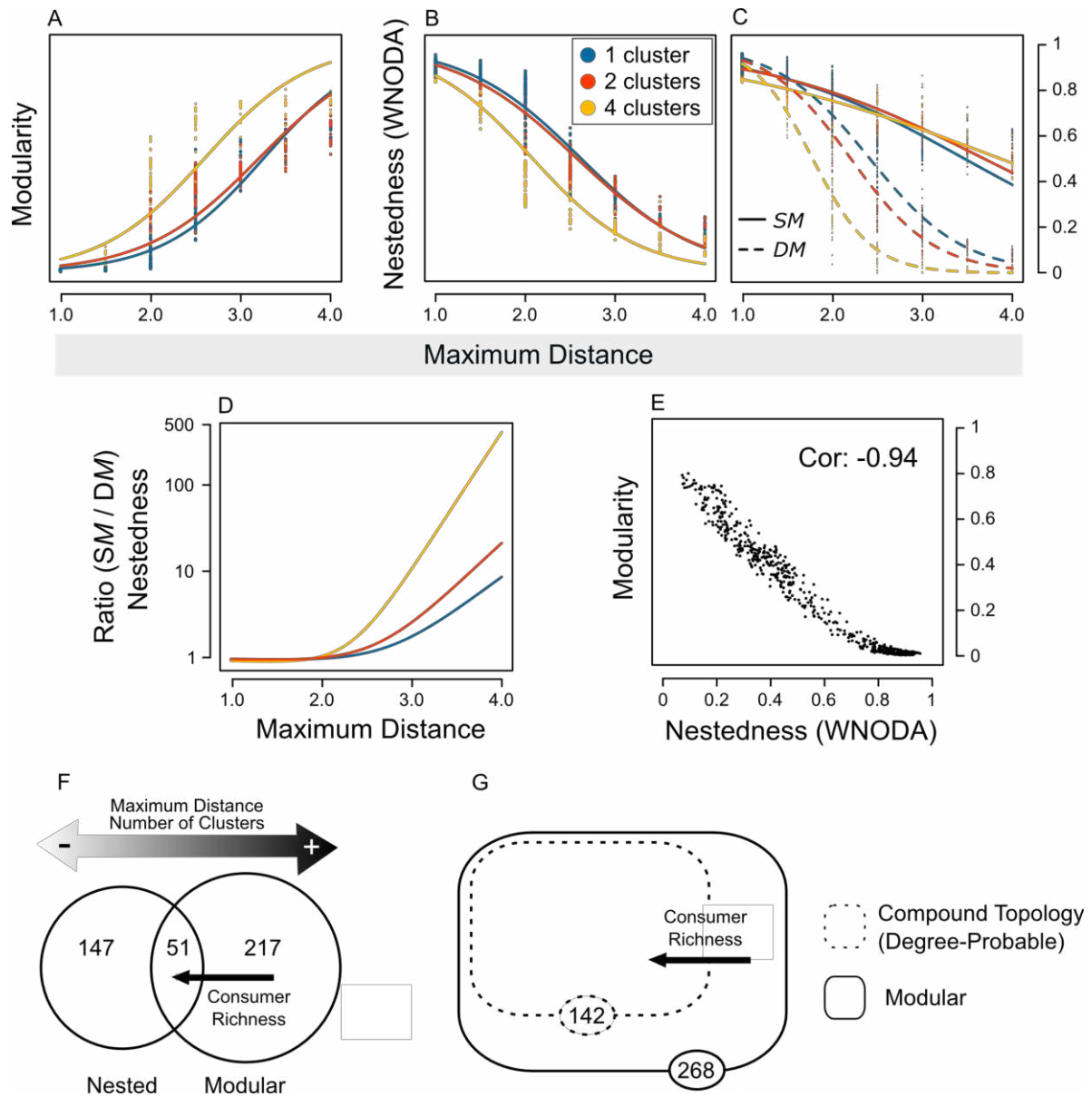


505

506 **Figure 4 – Network specialization metrics.** Connectance and H_2' are presented as a function
507 of maximum distance (horizontal axis), number of clusters (colors), and innate method
508 (columns of plots in the panel). The parameters represented are the ones with more explanatory
509 power in the generalized additive models (see Appendix S1.3-4). Average values of consumer
510 and resource species richness were used to draw the curves. Notice that plots are presented with
511 different scales in the horizontal axis.

512 From the 415 tested networks, 268 were significantly modular, 198 were significantly
513 nested, and 51 were both modular and nested. The probability of a network having a
514 modular topology increased with maximum distance and number of clusters, although
515 the chance of a network being nested is affected by both parameters on the opposite
516 direction. High consumer richness increased the chance of a simulated network being
517 nested, but had a minor effect on the chance of it being modular. The other parameters
518 had small effects on the models (Fig. 5F). Using the Equiprobable algorithm to define
519 the *a priori* probabilities in the restricted null models, we detected that all modular
520 networks showed in fact a compound topology. However, when the *a priori*
521 probabilities were based on node degrees (Degree-probable), from the 268 modular
522 networks, 142 were detected as having a compound topology. Using this last method,
523 the main factor affecting the chance of a modular network presenting a compound
524 topology was consumer richness. (Fig. 5G). For details see Appendix S1.9.

525



526

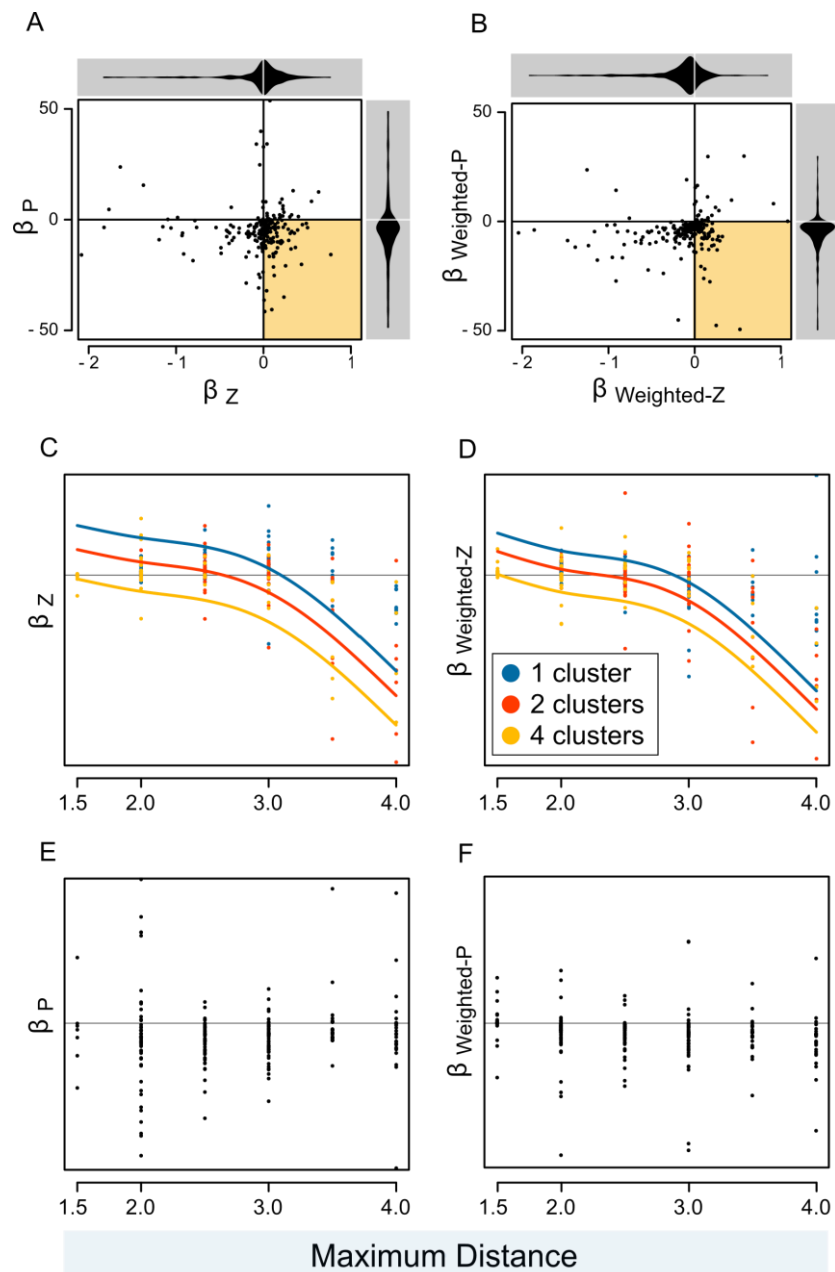
527 **Figure 5 – Simulation parameters affecting network topology.** (A) and (B) show the effect
 528 of maximum distance and number of clusters on modularity and nestedness of the simulated
 529 networks, respectively. Values of WNODA were divided by 100, resulting in values between 0
 530 and 1. In (C) nestedness is decomposed in its two components: nestedness between nodes of the
 531 same module ($WNODA_{SM}$, solid lines) and nestedness between nodes of different modules
 532 ($WNODA_{DM}$, dashed lines). Average values of consumer and resource richness were used to
 533 draw the curves in (A-C). Plot (D) shows the ratio between the expected $WNODA_{SM}$ and
 534 $WNODA_{DM}$ (curves on C) as a function of maximum distance. Notice that the vertical axis in D
 535 is log-transformed. In (E) a plot with nestedness vs. modularity shows the strong negative
 536 correlation between those metrics (Spearman correlation presented). (F) and (G) present Venn
 537 diagrams for network topologies and arrows for the main factors affecting the chance of a
 538 network showing each topology. The networks were classified as nested or modular based on
 539 null model analysis. Maximum distance and number of clusters have opposite effects on the
 540 chance of a network being nested or modular. Consumer richness had a strong effect on the
 541 probability of a network being nested, but a weak effect on its probability of being modular (F).
 542 Therefore, modular networks with high consumer richness have higher chance of also being

543 nested. We tested whether each modular network presented a compound topology using
544 restricted null models with two different methods to define *a priori* probabilities: equiprobable
545 and degree-probable. All modular networks were detected as having compound topologies by
546 the equiprobable restricted null model (not shown in the figure) and 142 were detected as
547 having compound topologies by the degree-probable restricted null model (G). In this latter
548 case, consumer species richness was the main factor influencing the probability of a modular
549 network having internally nested modules (compound topology). All results presented here were
550 obtained by fitting generalized linear models, except for (E), which was based on a Spearman
551 correlation. Complete results are presented in Appendix S1.

552

553 Most values of the β_P and $\beta_{\text{Weighted-P}}$ in the regressions with mean performance were
554 negative. However, this was not a ubiquitous pattern, as several positive values were
555 also found. For Z the results were still more diverse, since most of the β_Z values were
556 negative, although most of the $\beta_{\text{Weighted-Z}}$ values were positive (Fig. 6A-B). In general,
557 we found that the relationship between mean performance and Z decreased with
558 maximum distance and number of clusters (Fig. 6D-F), although the relationship
559 between mean performance and P was little or not affected by these parameters (Fig. G-
560 I). The same general trends were found in the analysis using maximum performance
561 instead of mean performance (Appendix S1.10). Similarly, most of the β_P and $\beta_{\text{Weighted-P}}$
562 values in the regressions with total performance were also negative, and $\beta_{\text{Weighted-Z}}$
563 values decreased with maximum distance, although this relationship was not observed
564 for β_Z (Appendix S1.10).

565



566

567 **Figure 6 - Simulation parameters affecting the multi-scale relationship between**
 568 **consumer's mean performance and specialization.** First, for each network we performed a
 569 linear regression between consumers' mean performance as a function of Z (within-module
 570 degree) and P (participation coefficient). In (A) we plotted the coefficients (β) of these
 571 regressions. We also performed this same procedure using weighted versions of Z and P (B).
 572 The colored region of (A) and (B) represents the multi-scale relationship between performance
 573 and specialization predicted by the IHS: negative within-module ($\beta_Z > 0$) and positive between-
 574 modules ($\beta_P < 0$). Notice that the values of Z and P are negatively related to specialization. We
 575 built generalized additive models to test for a relationship between regression coefficients and
 576 simulation parameters (Appendix S1). In (C-F) we present the regression coefficients as a
 577 function of maximum distance (horizontal axis) and number of clusters (colors) when it has a
 578 statistically significant effect on the model. There were some coefficients with extreme values,
 579 whose inclusion would make it difficult to visualize the plots, and so, we show only the core

580 region of each plot including most of the points and the predicted curves. Average values of
581 consumer and resource richness were used to draw the curves.

582

583 **Discussion**

584 The IHS model, following three first-principles, and through the adjustment of five
585 biologically meaningful parameters, has successfully produced a highly diverse set of
586 synthetic consumer-resource networks. In those simulations, specialization varied
587 largely, and we found the main topologies observed in real-world interaction networks:
588 nested, modular, and compound. We also found positive, neutral, and negative
589 relationships between consumers' performance and specialization, as well as multi-scale
590 relationships. Despite this not being the first theoretical model to produce or predict one
591 of those features separately (e.g., modularity: Guimerà *et al.* 2010; compound topology:
592 Leung & Weitz 2016; positive relationship between performance and specialization:
593 trade-off hypothesis, Poulin 1998; negative relationship between performance and
594 specialization: resource breadth hypothesis, Hellgren *et al.* 2009), as far as we know,
595 our model is the first to implement a single mechanism able to generate all patterns
596 under different circumstances.

597 It is important to notice that no network-level structure was imposed on our model or
598 emerged through network-level selection, but rather emerged from the rules on the
599 evolution of links between consumers and resources. Moreover, by comparing
600 simulated networks generated with different parameter setups we were able to identify
601 general contexts that are related to the emergence of each pattern.

602 **Model parameters and simulated networks**

603 Out of the five model parameters, maximum distance and number of clusters have
604 disproportionately affected the simulated networks. Maximum distance is linked to the
605 existence and intensity of trade-offs in consumer performances on different resources
606 and number of clusters affects how discontinuously are those trade-offs distributed in
607 the resource community. We found that discontinuities tend to reinforce the effect of
608 increasing trade-offs on network architecture (i.e. maximum distance and number of
609 clusters usually affect metrics of the simulated networks in the same direction).

610 The innate method defines the initial state of the network (the realized performance
611 matrix before the simulation), however it had weak effect in most of the analysis of
612 simulated networks (the realized performance matrix after the simulation), which shows
613 that consumer evolution was strong enough to overcome initial patterns in most
614 simulations. The only metric that was strongly driven by innate method was the
615 proportion of iterations in which occurred evolutionary changes (for a discussion of this
616 result, see Appendix S1.1). Overall, consumer and resource richness did not strongly

617 influence the simulation outputs either, being important just in some analyses (e.g.,
618 compound topology), which we discuss further.

619 When using the IHS model, it is imperative to keep in mind that the simulated networks
620 are ideal networks and several weak links on the matrices may not be detected in
621 empirical studies or even may not happen in nature. First, it is well recognized that
622 weak interactions are unlikely to be sampled in ecological studies (Jordano 2016).
623 Also, some links may be so weak that it does not happen even once in ecological time
624 or the resource exploitation is avoided by the consumer because it does not compensate
625 the energy costs. For last, in most of interaction networks, weights are measured as
626 counts (e.g. abundance of parasites in hosts, floral visits of pollinators), thus, imposing a
627 lower limit on link weights (a link lower than 1 cannot occur). Therefore, despite
628 several simulated networks have very high connectance, this is not likely to be found in
629 empirical studies.

630 **Trade-offs and specialization**

631 In general, higher values of maximum distance and number of clusters resulted in
632 specialist consumers having higher performance than generalists on each resource, and
633 in more specialized, more modular and less nested simulated networks. When trade-offs
634 are strong, the jack-of-all-trades is master of none or, even, does not exist, and the
635 network is sparse, with several forbidden links. However, when trade-offs are weak, the
636 jack-of-all-trades is master of all, and the network is highly connected. When there is no
637 trade-off at all (no distance between resources greater than 1), there is no forbidden
638 links and connectance is always 1.

639 In natural systems we may expect that the intensity of trade-offs depends on the type
640 and intimacy of the studied ecological interaction. As more intimate interactions require
641 stronger match between interacting species than less intimate interactions (Hembry *et*
642 *al.* 2018), the same difference between two resource species, tends to represent a
643 stronger trade-off in intimate networks. For instance, slight physiological differences
644 between two resources may strongly affect the probability of each resource being
645 exploited by a given endoparasite, but be irrelevant to their probabilities of being preyed
646 upon. In agreement with our predictions, ecological interactions known to be more
647 intimate usually are more specialized than less intimate interactions (e.g., pollination *vs.*
648 seed dispersal, Blüthgen *et al.* 2007; parasitism and parasitoidism *vs.* predatism, Van
649 Veen *et al.* 2008; leaf mining *vs.* leaf chewing, Novotny *et al.* 2010), and form sparsely
650 connected and modular networks, although low intimacy leads to highly connected and
651 nested networks (Guimarães *et al.* 2007a; Pires & Guimaraes 2012; Hembry *et al.*
652 2018).

653 One of the most pervasive patterns in ecological networks is a negative relationship
654 between size and connectance (Jordano 1987; Blüthgen *et al.* 2007). However, in our
655 simulated networks, connectance was just minimally affected by consumer and resource
656 richness (i.e., network size), but mostly driven by the intensity of trade-offs. Our results

657 suggest that connectance in real-world ecological networks is not directly related to
658 network size, but a consequence of larger networks usually comprising a more
659 heterogeneous set of organisms and, therefore, containing stronger trade-offs. The same
660 may hold for other network features that are affected by the intensity of trade-offs, such
661 as modularity and nestedness. Using a similar rationale, Jordano (1987) argues that
662 larger seed-dispersal networks are more compartmentalized and less connected because
663 they include more diverse sets of feeding structures and fruit types. Moreover, Flores *et*
664 *al.* (2011), in a set of nested networks, did not find a relationship between connectance
665 and size, and Montoya *et al.* (2015) found that modularity in island networks was
666 related with functional diversity but not with species richness, both corroborating that
667 specialization decreases with heterogeneity and not with size itself.

668 **Compound topology**

669 On the one hand, several simulated networks presented both significant nestedness and
670 modularity. On the other hand, nestedness and modularity are driven in opposite
671 directions by the same main parameters (maximum distance and number of clusters)
672 and are strongly negatively correlated, as usually found in empirical ecological
673 networks (Thebault & Fontaine 2010; Pires & Guimaraes 2012; Trøjelsgaard & Olesen
674 2013). This scenario does not support the perspective of the overall network having a
675 mixed nested and modular structure (Fortuna *et al.* 2010), but is consonant with the
676 perspective that each topology may predominate at different network scales (Felix *et al.*
677 2017).

678 Indeed, in modular-nested simulated networks, most of network nestedness came from
679 the smaller scale: $WNODA_{SM}$ was always much higher than $WNODA_{DM}$. Our model
680 predicts that networks without trade-offs should present a nested topology, and
681 reinforces the prediction that highly diverse networks tend to present a compound
682 topology (Lewinsohn *et al.* 2006; Flores *et al.* 2011; Felix *et al.* 2017). In these
683 networks, consumers tend to specialize in a group of homogeneous resource species
684 instead of a single species (Fig. 2D), which corroborates that network modules may be
685 the real unity of specialization and coevolution (Olesen *et al.* 2007). Recently, as a
686 result of conceptual and methodological improvements in ecological network science,
687 compound topologies have been detected in several real-world networks that could be
688 previously classified as purely modular or nested-modular (Flores *et al.* 2013; Felix *et*
689 *al.* 2017; Solé-Ribalta *et al.* 2018).

690 We did not find a ubiquitous multi-scale relationship between consumer performance
691 and specialization in modular networks, which suggests that this previously predicted
692 pattern (Pinheiro *et al.* 2016) that has already been observed in nature (Felix *et al.*
693 2017), is not a necessary consequence of the IHS, but one of the possible structures that
694 may emerge in diverse consumer-resource interaction systems. When the trade-offs are
695 too strong, a positive relationship between performance and specialization emerges even
696 within modules, which leads to extreme specialization. These are the situations in which
697 we should expect to find pairwise specialization and coevolution. The relationship

698 between performance and specialization in different modules presented a more random
699 variation, that could not be explained based on the intensity of trade-offs in the
700 simulations. If, on the one hand, a multi-scale relationship in modular networks was
701 found in just a few cases, on the other hand, when entire simulated networks with
702 increasing resource diversity are compared to one another, there is a clear inversion in
703 the expected relationship between consumer performance and specialization.

704 Our results show that scale is key to understand the architecture and dynamics of
705 ecological networks. And by scale we mean the hierarchical levels within a given
706 network (e.g., network, modules, nodes), and the different taxonomic, phylogenetic,
707 functional, and geographic scales that may be sampled when building a network from
708 empirical data. Interaction networks containing only similar species show patterns that
709 are not observed in more heterogeneous networks, as well as a module does not reflect
710 the structure of the entire network. And, as previously commented by other authors,
711 studies of ecological interactions are usually focused on modules of the network or in
712 taxonomically defined assemblages subsets (Olesen *et al.* 2007; Jordano 2016). Thus,
713 the literature is probably biased towards low-scale patterns (as suggested by Bezerra *et*
714 *al.* 2009; Mello *et al.* 2011). This may explain, for instance, the paradigm of mutualism
715 being always nested (Bascompte & Jordano 2007) and the dominance of positive
716 relationships between performance and host range of parasites in the literature (Krasnov
717 *et al.* 2004; Hellgren *et al.* 2009). Moreover, we may expect that several of the
718 published nested interaction networks are in fact modules of more complete networks
719 with compound topologies.

720 **Competing models that produce compound topologies**

721 Beckett & Williams (2013) have predicted a compound topology for phage-bacteria
722 networks, using a relaxed lock-and-key model. Despite their model including a larger
723 number of parameters and having a more complex and less general mechanism than
724 ours, most principles of the IHS model are at least partially met by it. In fact, only the
725 first-principle (iii) of our model is not mirrored in some extent by their model, since
726 performance is not defined only by consumer evolution, but also by resource evolution.
727 We believe that our model is not contradictory to the relaxed lock-and-key model, but
728 rather more comprehensive. Generality gets more and more important in those models,
729 as observations of compound topologies in other systems are made (Felix *et al.* 2017;
730 Solé-Ribalta *et al.* 2018).

731 Leung & Weitz (2016) proposed a bipartite network growth model that can also produce
732 modular, nested, and compound networks. The mechanics of their model is very
733 different from ours, mainly in two major aspects. First, in their model, a network grows
734 by duplication of nodes, while in our model the number of species in the system is kept
735 constant. Second, in their model once a link is established between two nodes it is not
736 modified anymore, while in our model links depends on the match between consumers
737 and resources, which is subjected to evolution. Moreover, contrary to the IHS model,
738 their model produces only binary networks. These differences make it very difficult to

739 compare assumptions and mechanisms of both models. However, it is remarkable that
740 Leung & Weitz (2016) found that, when there are trade-offs, modularity emerges in
741 networks, otherwise, hosts and parasites enter an arms race that results in nestedness.
742 This is highly consonant with our main predictions using the IHS model.

743 **Limitations of the model**

744 The main limitation of the IHS model is the assumption that innate performance is
745 modified only by the evolution of consumer species. In nature, consumption is likely to
746 be a selective force that also drives resource species evolution (Thompson 1994). This
747 limitation is especially important in mutualisms, where it is not trivial to classify each
748 partner as consumer or resource. In these cases, application of our model should take
749 into account the available knowledge about the evolution of the species groups involved
750 in the interaction. For instance, in pollination systems we may be eager to classify
751 animals as consumers and plants as resources, because of the trophic relationship
752 between them. However, there is strong evidence that plants evolve in response to
753 pollinator-mediated selection, although the opposite is seldom true (Armbruster 2017).
754 Therefore, it may be more appropriate to consider pollinators as resources exploited by
755 plants in order to reproduce.

756 Another relevant limitation of our model is that the realized performance is determined
757 only by resource species carrying capacity and innate performance, and does not
758 consider consumer species abundance. This is a direct consequence of the IHS being
759 initially proposed inspired by endoparasitic interactions. In obligatory interactions, from
760 the consumers' perspective, mainly when they are symbiotic, the abundance of the
761 consumer species is itself a measure of interaction weight, as the consumer only
762 survives by interacting. Then it is reasonable to consider consumer abundance and
763 performance together in the model. However, in facultative interactions, in which
764 consumer abundance is less dependent on the interaction, to not consider the separated
765 effect of abundance and trait-matching in link establishment may represent a strong
766 caveat.

767 Other limitations of the IHS model are: (1) the model does not include extinctions nor
768 cladogenesis. It is important to warn that the present model does not aim to explain
769 species coexistence in an ecological system but assumes it *a priori*. (2) The consumer-
770 resource system is assumed to be closed: there is no emigration or immigration; and (3)
771 links are affected just by the match between consumer and resource, overlooking factors
772 exogenous to the species that may affect link establishment, e.g., context dependence
773 (Chamberlain *et al.* 2014). Nevertheless, despite these somewhat simplistic
774 assumptions, our model was able to recover all common topological patterns observed
775 among interaction networks.

776 **Conclusion**

777 In summary, we propose a new model for generating consumer-resource networks
778 based on the integrative hypothesis of specialization (IHS). Despite its limitations,
779 which are inherent to a model aiming at generality, our model may be a useful source of
780 testable predictions.

781 One great challenge ahead is to parameterize our model based on real-world data, in
782 order to generate more precise and quantitative predictions for particular kinds of
783 networks. This is no simple task, though, as the distance between resource species is a
784 non-dimensional variable, based on an abstract concept, which is affected by several
785 factors. One possible solution would be to develop proxies for resource species
786 distances based on phylogenetic, trait-based, or interaction-based distances.

787 However, even without these refinements, the proposed model reproduced several
788 already observed patterns and most of its predictions are coherent to real-world
789 observations and consonant with current evolutionary and ecological theories. Our
790 results show that the IHS model is useful to generate synthetic, weighted, bipartite,
791 consumer-resource networks and supports the IHS as a theoretical framework to study
792 interaction specialization and network topology.

793 **Acknowledgements:**

794 We thank our institutions and many colleagues, who helped us in different ways during
795 this project. We thank J. Miguel Ortega, Tetsu Sakamoto, and Verônica de Melo Costa
796 for help with the use of Sagarana HPC cluster. The Graduate School in Ecology of the
797 Federal University of Minas Gerais (ECMVS), Brazil, provided us with a scholarship
798 from the Brazilian Council for Scientific and Technological Development (CNPq)
799 granted to RBPP. Infrastructure for this study was provided by ECMVS, the
800 Department of Ecology of the University of São Paulo (USP), and the Department of
801 Biometry and Environmental System Analysis, University of Freiburg, Germany. The
802 Graduate School in Ecology of the State University of Campinas (PPGE-UNICAMP),
803 Brazil, provided GMFF with a scholarship from the Brazilian Coordination for the
804 Improvement of Higher Education Personnel (CAPES). RBPP received a scholarship
805 from the joint program between CAPES, CNPq, and Deutscher Akademischer
806 Austauschdienst (DAAD) (88887.161398/2017-00) to make a one-year sandwich Ph.D
807 at the University of Freiburg. MARM was funded by the Minas Gerais Research
808 Foundation (FAPEMIG #PPM-00324-15), the Alexander von Humboldt Foundation
809 (AvH: 3.4-8151/15037), and CNPq (#302700/2016-1).

810 **Authorship:**

811 All authors contributed to model development and study design. RBPP coded the model
812 and performed the statistical analysis. All authors contributed to the interpretation of
813 results. RBPP wrote the first draft and all authors reviewed the manuscript.

814

815 **References**

- 816 Almeida-Neto, M., Guimarães, P., Guimarães, P.R., Loyola, R.D. & Ulrich, W. (2008).
817 A consistent metric for nestedness analysis in ecological systems: reconciling
818 concept and measurement. *Oikos*, 117, 1227–1239.
- 819 Almeida-Neto, M. & Ulrich, W. (2011). A straightforward computational approach for
820 measuring nestedness using quantitative matrices. *Environ. Model. Softw.*, 26,
821 173–178.
- 822 Armbruster, W.S. (2017). The specialization continuum in pollination systems:
823 diversity of concepts and implications for ecology, evolution and conservation.
824 *Funct. Ecol.*, 31, 88–100.
- 825 Barber, M.J. (2007). Modularity and community detection in bipartite networks. *Phys.*
826 *Rev. E*, 76, 066102.
- 827 Bascompte, J. & Jordano, P. (2007). Plant-animal mutualistic networks: the architecture
828 of biodiversity. *Annu. Rev. Ecol. Evol. Syst.*, 38, 567–593.
- 829 Bascompte, J., Jordano, P., Melian, C.J. & Olesen, J.M. (2003). The nested assembly of
830 plant-animal mutualistic networks. *Proc. Natl. Acad. Sci.*, 100, 9383–9387.
- 831 Beckett, S.J. (2016). Improved community detection in weighted bipartite networks. *R.*
832 *Soc. Open Sci.*, 3, 140536.
- 833 Beckett, S.J. & Williams, H.T.P. (2013). Coevolutionary diversification creates nested-
834 modular structure in phage-bacteria interaction networks. *Interface Focus*, 3,
835 20130033–20130033.
- 836 Bellay, S., Lima, D.P., Takemoto, R.M. & Luque, J.L. (2011). A host-endoparasite
837 network of Neotropical marine fish: are there organizational patterns?
838 *Parasitology*, 138, 1945–1952.
- 839 Bezerra, E.L.S., Machado, I.C. & Mello, M.A.R. (2009). Pollination networks of oil-
840 flowers: a tiny world within the smallest of all worlds. *J. Anim. Ecol.*, 78, 1096–
841 1101.
- 842 Blüthgen, N., Menzel, F. & Blüthgen, N. (2006). Measuring specialization in species
843 interaction networks. *BMC Ecol.*, 6, 9.
- 844 Blüthgen, N., Menzel, F., Hovestadt, T., Fiala, B. & Blüthgen, N. (2007).
845 Specialization, constraints, and conflicting interests in mutualistic networks. *Curr.*
846 *Biol.*, 17, 341–346.
- 847 Chamberlain, S.A., Bronstein, J.L. & Rudgers, J.A. (2014). How context dependent are
848 species interactions? *Ecol. Lett.*, 17, 881–890.
- 849 Donatti, C.I., Guimarães, P.R., Galetti, M., Pizo, M.A., Marquitti, F.M.D. & Dirzo, R.
850 (2011). Analysis of a hyper-diverse seed dispersal network: modularity and
851 underlying mechanisms. *Ecol. Lett.*, 14, 773–781.

- 852 Dormann, C.F., Fründ, J. & Schaefer, H.M. (2017). Identifying causes of patterns in
853 ecological networks: opportunities and limitations. *Annu. Rev. Ecol. Evol. Syst.*,
854 48, 559–584.
- 855 Dormann, C.F., Gruber, B. & Fründ, J. (2008). Introducing the bipartite Package:
856 Analysing Ecological Networks. *R News*, 8, 8–11.
- 857 Felix, G.M., Pinheiro, R.B.P., Poulin, R., Krasnov, B.R. & Mello, M.A.R. (2017). The
858 compound topology of a continent-wide interaction network explained by an
859 integrative hypothesis of specialization. *bioRxiv*.
- 860 Flores, C.O., Meyer, J.R., Valverde, S., Farr, L. & Weitz, J.S. (2011). Statistical
861 structure of host-phage interactions. *Proc. Natl. Acad. Sci.*, 108, E288–E297.
- 862 Flores, C.O., Valverde, S. & Weitz, J.S. (2013). Multi-scale structure and geographic
863 drivers of cross-infection within marine bacteria and phages. *ISME J.*, 7, 520–532.
- 864 Fortuna, M.A., Stouffer, D.B., Olesen, J.M., Jordano, P., Mouillot, D., Krasnov, B.R., *et*
865 *al.* (2010). Nestedness versus modularity in ecological networks: two sides of the
866 same coin? *J. Anim. Ecol.*, 79, 811–817.
- 867 Futuyma, D.J. & Moreno, G. (1988). The evolution of ecological specialization. *Annu.*
868 *Rev. Ecol. Syst.*, 19, 207–233.
- 869 García-Robledo, C. & Horvitz, C.C. (2012). Jack of all trades masters novel host plants:
870 positive genetic correlations in specialist and generalist insect herbivores
871 expanding their diets to novel hosts. *J. Evol. Biol.*, 25, 38–53.
- 872 Guimarães, P.R., Rico-Gray, V., Oliveira, P.S., Izzo, T.J., dos Reis, S.F. & Thompson,
873 J.N. (2007a). Interaction intimacy affects structure and coevolutionary dynamics in
874 mutualistic networks. *Curr. Biol.*, 17, 1797–1803.
- 875 Guimarães, P.R., Sazima, C., Reis, S.F. d. & Sazima, I. (2007b). The nested structure of
876 marine cleaning symbiosis: is it like flowers and bees? *Biol. Lett.*, 3, 51–54.
- 877 Guimerà, R. & Nunes Amaral, L.A. (2005). Functional cartography of complex
878 metabolic networks. *Nature*, 433, 895–900.
- 879 Guimerà, R., Stouffer, D.B., Sales-Pardo, M., Leicht, E.A., Newman, M.E.J. & Amaral,
880 L.A.N. (2010). Origin of compartmentalization in food webs. *Ecology*, 91, 2941–
881 2951.
- 882 Hellgren, O., Pérez-Tris, J. & Bensch, S. (2009). A jack-of-all-trades and still a master
883 of some: prevalence and host range in avian malaria and related blood parasites.
884 *Ecology*, 90, 2840–2849.
- 885 Hembry, D.H., Raimundo, R.L.G., Newman, E.A., Atkinson, L., Guo, C., Guimarães,
886 P.R., *et al.* (2018). Does biological intimacy shape ecological network structure? A
887 test using a brood pollination mutualism on continental and oceanic islands. *J.*
888 *Anim. Ecol.*, 0–2.
- 889 Ings, T.C., Montoya, J.M., Bascompte, J., Blüthgen, N., Brown, L., Dormann, C.F., *et*

- 890 *al.* (2009). Ecological networks - Beyond food webs. *J. Anim. Ecol.*, 78, 253–269.
- 891 Jordano, P. (1987). Patterns of mutualistic interactions in pollination and seed dispersal:
892 connectance, dependence asymmetries, and coevolution. *Am. Nat.*, 129, 657–677.
- 893 Jordano, P. (2016). Sampling networks of ecological interactions. *Funct. Ecol.*, 30,
894 1883–1893.
- 895 Krasnov, B.R., Fortuna, M.A., Mouillot, D., Khokhlova, I.S., Shenbrot, G.I. & Poulin,
896 R. (2012). Phylogenetic signal in module composition and species connectivity in
897 compartmentalized host-parasite Networks. *Am. Nat.*, 179, 501–511.
- 898 Krasnov, B.R., Poulin, R., Shenbrot, G.I., Mouillot, D. & Khokhlova, I.S. (2004).
899 Ectoparasitic “jacks-of-all-trades”: relationship between abundance and host
900 specificity in fleas (Siphonaptera) parasitic on small mammals. *Am. Nat.*, 164,
901 506–516.
- 902 Krishna, A., Guimarães Jr, P.R., Jordano, P. & Bascompte, J. (2008). A neutral-niche
903 theory of nestedness in mutualistic networks. *Oikos*, 117, 1609–1618.
- 904 Leung, C.Y. (Joey) & Weitz, J.S. (2016). Conflicting attachment and the growth of
905 bipartite networks. *Phys. Rev. E*, 93, 032303.
- 906 Lewinsohn, T.M., Inácio Prado, P., Jordano, P., Bascompte, J. & M. Olesen, J. (2006).
907 Structure in plant-animal interaction assemblages. *Oikos*, 113, 174–184.
- 908 Mello, M.A.R., Marquitti, F.M.D., Guimarães, P.R., Kalko, E.K.V., Jordano, P. & de
909 Aguiar, M.A.M. (2011). The modularity of seed dispersal: differences in structure
910 and robustness between bat– and bird–fruit networks. *Oecologia*, 167, 131–140.
- 911 Montoya, D., Yallop, M.L. & Memmott, J. (2015). Functional group diversity increases
912 with modularity in complex food webs. *Nat. Commun.*, 6, 7379.
- 913 Muchhala, N. (2007). Adaptive trade-off in floral morphology mediates specialization
914 for flowers pollinated by bats and hummingbirds. *Am. Nat.*, 169, 494–504.
- 915 Novotny, V., Miller, S.E., Baje, L., Balagawi, S., Basset, Y., Cizek, L., *et al.* (2010).
916 Guild-specific patterns of species richness and host specialization in plant-
917 herbivore food webs from a tropical forest. *J. Anim. Ecol.*, 79, 1193–1203.
- 918 Olesen, J.M., Bascompte, J., Dupont, Y.L. & Jordano, P. (2007). The modularity of
919 pollination networks. *Proc. Natl. Acad. Sci. U. S. A.*, 104, 19891–19896.
- 920 Pinheiro, R.B.P., Félix, G.M.F., Chaves, A. V., Lacorte, G.A., Santos, F.R., Braga,
921 É.M., *et al.* (2016). Trade-offs and resource breadth processes as drivers of
922 performance and specificity in a host–parasite system: a new integrative
923 hypothesis. *Int. J. Parasitol.*, 46, 115–121.
- 924 Pires, M.M. & Guimaraes, P.R. (2012). Interaction intimacy organizes networks of
925 antagonistic interactions in different ways. *J. R. Soc. Interface*, 10, 20120649–
926 20120649.

- 927 Poisot, T., Canard, E., Mouquet, N. & Hochberg, M.E. (2012). A comparative study of
928 ecological specialization estimators. *Methods Ecol. Evol.*, 3, 537–544.
- 929 Poulin, R. (1998). Large-scale patterns of host use by parasites of freshwater fishes.
930 *Ecol. Lett.*, 1, 118–128.
- 931 R Core Team (2017). R: A language and environment for statistical computing. R
932 Foundation for Statistical Computing, Vienna, Austria. URL [https://www.R-](https://www.R-project.org/)
933 [project.org/](https://www.R-project.org/)
- 934 Servedio, M.R., Brandvain, Y., Dhole, S., Fitzpatrick, C.L., Goldberg, E.E., Stern, C.A.,
935 *et al.* (2014). Not just a theory - The utility of mathematical models in evolutionary
936 biology. *PLoS Biol.*, 12, e1002017.
- 937 Solé-Ribalta, A., Tessone, C.J., Mariani, M.S. & Borge-Holthoefer, J. (2018).
938 Revealing in-block nestedness: Detection and benchmarking. *Phys. Rev. E*, 97,
939 062302.
- 940 Stang, M., Klinkhamer, P.G.L. & van der Meijden, E. (2007). Asymmetric
941 specialization and extinction risk in plant–flower visitor webs: a matter of
942 morphology or abundance? *Oecologia*, 151, 442–453.
- 943 Thebault, E. & Fontaine, C. (2010). Stability of ecological communities and the
944 architecture of mutualistic and trophic networks. *Science (80-.)*, 329, 853–856.
- 945 Thompson, J.N. (1994). *The coevolutionary process*. University of Chicago Press,
946 Chicago, USA.
- 947 Trøjelsgaard, K. & Olesen, J.M. (2013). Macroecology of pollination networks. *Glob.*
948 *Ecol. Biogeogr.*, 22, 149–162.
- 949 Ulrich, W., Kryszewski, W., Sewerniak, P., Puchałka, R., Strona, G. & Gotelli, N.J.
950 (2017). A comprehensive framework for the study of species co-occurrences,
951 nestedness and turnover. *Oikos*, 1607–1616.
- 952 Vázquez, D.P., J. Melián, C., M. Williams, N., Blüthgen, N., R. Krasnov, B. & Poulin,
953 R. (2007). Species abundance and asymmetric interaction strength in ecological
954 networks. *Oikos*, 116, 1120–1127.
- 955 Van Veen, F.J.F., Müller, C.B., Pell, J.K. & Godfray, H.C.J. (2008). Food web structure
956 of three guilds of natural enemies: predators, parasitoids and pathogens of aphids.
957 *J. Anim. Ecol.*, 77, 191–200.
- 958 Watts, S., Dormann, C.F., Martín González, A.M. & Ollerton, J. (2016). The influence
959 of floral traits on specialization and modularity of plant–pollinator networks in a
960 biodiversity hotspot in the Peruvian Andes. *Ann. Bot.*, 118, 415–429.
- 961
- 962
- 963

964 **Supporting Information**

965 Figure S1 - An example of one iteration of the IHS model.

966 Supplement S1 - Code for the IHS model (ZIP file).

967 Supplement S2 - R function nest.smdm (ZIP file).

968 Appendix S1 - Supplementary analysis.

969 Appendix S2 - Weighted nestedness based on overlap and decreasing abundance
970 (WNODA)